



HAL
open science

Determination of hydrogen peroxide by differential pulse polarography in advanced oxidation processes for water treatment

Lionel Domergue, Nicolas Cimetiere, Sylvain Giraudet, Didier Hauchard

► **To cite this version:**

Lionel Domergue, Nicolas Cimetiere, Sylvain Giraudet, Didier Hauchard. Determination of hydrogen peroxide by differential pulse polarography in advanced oxidation processes for water treatment. *Journal of Water Process Engineering*, 2023, 53, pp.103707. 10.1016/j.jwpe.2023.103707 . hal-04115736

HAL Id: hal-04115736

<https://hal.science/hal-04115736>

Submitted on 19 Sep 2023

HAL is a multi-disciplinary open access archive for the deposit and dissemination of scientific research documents, whether they are published or not. The documents may come from teaching and research institutions in France or abroad, or from public or private research centers.

L'archive ouverte pluridisciplinaire **HAL**, est destinée au dépôt et à la diffusion de documents scientifiques de niveau recherche, publiés ou non, émanant des établissements d'enseignement et de recherche français ou étrangers, des laboratoires publics ou privés.

1 Highlights

2 **Determination of hydrogen peroxide by differential pulse polarogra-**
3 **phy in advanced oxidation processes for water treatment**

4 Lionel Domergue, Nicolas Cimetière, Sylvain Giraudet, Didier Hauchard

- 5 • Quantification of residual H_2O_2 in Fenton and electro-Fenton processes
- 6 • Calibration range of H_2O_2 between 0.02 to 1.00 mmol L^{-1}
- 7 • Limit of detection and quantification respectively 13 and 21 $\mu\text{mol L}^{-1}$
- 8 • No interference from Fe^{3+} or dissolved O_2
- 9 • Overestimate of the measurement by the presence of Zn^{2+} in solution

10 Determination of hydrogen peroxide by differential
11 pulse polarography in advanced oxidation processes for
12 water treatment

13 Lionel Domergue^{a,*}, Nicolas Cimetière^a, Sylvain Giraudet^a, Didier Hauchard^a

14 ^aUniv Rennes, École Nationale Supérieure de Chimie de Rennes, CNRS, ISCR (Institut des
15 Sciences Chimiques de Rennes) – UMR 6226, F-35000 Rennes, France

16 **Abstract**

17 Knowing the concentration of hydrogen peroxide (H_2O_2) is crucial for the mon-
18 itoring and optimizing the Fenton reaction in advanced oxidation processes.
19 Several analytical methods exist to determine these concentrations, but their
20 applications can be difficult because of low selectivity (interaction with other
21 metals), the use of toxic compounds, or low concentrations ($\mu\text{mol L}^{-1}$). To over-
22 come these problems, we developed a differential pulse polarographic (DPP)
23 method at the dropping mercury electrode (DME) with the following condi-
24 tions : $t_g = 1.0\text{ s}$, $\Delta E = -100\text{ mV}$ and $v = 10\text{ mV s}^{-1}$. Calibration curves
25 had very high correlation coefficients ($R^2 > 0.999$). The limits of detection
26 and quantification were evaluated respectively at 13 and 21 $\mu\text{mol L}^{-1}$ with peak
27 area measurements of hydrogen peroxide reduction (A_p). The DPP method
28 was compared with other analytical methods (iodometric titration and spec-
29 trophotometry) for determining at low concentrations of H_2O_2 (in the order of
30 mmol L^{-1} to $\mu\text{mol L}^{-1}$) in Fenton and electro-Fenton processes. The method
31 developed here allows measure low concentrations of hydrogen peroxide in Fen-
32 ton and electro-Fenton processes in acidic solutions pH (~ 3) and the presence
33 of interfering species such as Fe^{3+} and dissolved oxygen.

34 *Keywords:* differential pulse polarography, hydrogen peroxide, residual
35 concentrations, Fenton process, water treatment

*Corresponding author
Email address: lionel.domergue@ensc-rennes.fr (Lionel Domergue)
Preprint submitted to Journal of Water Process Engineering

36 1. Introduction

37 Advanced oxidation processes (AOPs) are innovative water and wastewater
38 treatments commonly used to eliminate various persistent organic pollutants
39 [1, 2, 3]. Hydrogen peroxide (H_2O_2) is a strong oxidant (standard potential $E^\circ =$
40 1.80 and $0.87 \text{ V}_{/\text{SHE}}$ at pH 0 and 14, respectively) that can be used directly as an
41 oxidizing agent [4] or as a mediator to generate stronger oxidants like hydroxyl
42 radicals (HO^\bullet , $E^\circ = 2.80 \text{ V}_{/\text{SHE}}$) [5, 6] in AOPs such as homogenous chemical
43 oxidation processes ($\text{H}_2\text{O}_2/\text{Fe}^{2+}$ and $\text{H}_2\text{O}_2/\text{O}_3$), homogeneous/heterogeneous
44 photocatalytic processes ($\text{H}_2\text{O}_2/\text{UV}$, and $\text{Fe}^{2+}/\text{H}_2\text{O}_2/\text{UV}$), and electro-Fenton
45 processes [7, 8, 9, 10]. The most common AOPs are based on the Fenton re-
46 action, which involves the oxidation of ferrous iron by hydrogen peroxide to
47 produce reactive hydroxyl radicals (eq. (1)) [4, 11] that degrade organic pollu-
48 tants.



49 In these AOPs, it is very important to control and monitor the H_2O_2 con-
50 centration, in particular in the electro-Fenton process where hydrogen peroxide
51 is continuously electro-generated by reduction of dissolved molecular oxygen at
52 the cathode [12, 13]. This continuous *in situ* H_2O_2 production requires the
53 analysis of low H_2O_2 concentrations ($100 \mu\text{mol L}^{-1}$ to 10 mmol L^{-1}). Several
54 non-enzymatic methods for determining hydrogen peroxide concentration in so-
55 lution have been reported [14, 15, 16]. However, although these methods can be
56 used in some cases, they are not adapted for the determination of low concentra-
57 tions of hydrogen peroxide in AOPs. For instance, iodometry uses the oxidizing
58 properties of H_2O_2 towards iodide ion to form iodine (as I_3^- complexes), which is
59 quantified by thiosulfate titration [17]. However, this method is only suitable for
60 high concentrations (higher than 1 mmol L^{-1}) and is not very selective (possible
61 interaction with metallic species and reaction with dissolved oxygen) [18]. An-
62 other method uses the redox reaction between H_2O_2 and Cu^{2+} in the presence
63 of 2,9-dimethyl-1,10-phenanthroline (DMP) [19]. In the complexometric DMP

64 titration method, yellow or orange complexes are produced and quantified by
65 spectrophotometry at 454.5 nm. However, the DMP method is only applicable
66 within a pH range of 4 to 10, which does not correspond to the conditions of the
67 Fenton reaction where the pH generally does not exceed 3 [20]. Another option
68 is to use the reaction between hydrogen peroxide and titanium chloride, which
69 produces a molecule pertitanic acid, that can be analysed with a UV-visible
70 spectrophotometer [21, 22]. The limit of detection with this method is very low
71 : $30 \mu\text{mol L}^{-1}$ [23]. This analytical method is selective but requires the use of
72 toxic reagent (titanium chloride) and spectrophotometric measurements require
73 clear solutions without turbidity.

74 Recently, others methods have been developed to determine H_2O_2 during
75 Fenton reactions. One of these use the oxidative coloration of 2,2'-azino-bis-
76 (3-ethylbenzothiazoline-6-sulfonate) (ABTS) via the Fenton reaction. With this
77 system, H_2O_2 concentration can be determined by multi-wavelength spectrophoto-
78 tometry with quite high sensitivity ($4.19 \times 10^4 \text{ L mol}^{-1} \text{ cm}^{-1}$ at 415 nm) and a
79 detection limit of $0.18 \mu\text{mol L}^{-1}$ [24]. Another spectrophotometric method was
80 developed for the determination of hydrogen peroxide in photo-Fenton processes.
81 This method is based on the reaction of H_2O_2 with ammonium metavanadate
82 in an acidic medium, which results in the formation of a red-orange peroxy-
83 vanadium cation, with a maximum absorbance at 450 nm. This method has a
84 detection limit of $143 \mu\text{mol L}^{-1}$ [25]. However, these methods are unsuitable for
85 the routine determination of H_2O_2 in the Fenton reaction because they require
86 the use of expensive products and complex multi-measurement methods.

Ever since the introduction of polarography by Heyrovsky [26], it has been known that hydrogen peroxide is reduced at the dropping mercury electrode (DME) (eq. (2)).



87 An inert gas, normally N_2 or H_2 , has to be passed for at least 10 to 15 min to
88 remove dissolved oxygen. Modern electro-analytical instrumentation especially
89 voltammetric techniques provide reliable and reproducible data for the quan-

90 tification of the analyte [27, 28]. The current peak intensity or the peak area
91 corresponding to the reduction of H_2O_2 must be proportional to the concentra-
92 tion of the analyte in solution and allows a quantitative analysis of the solute
93 [29]. To our knowledge, the polarographic reduction wave has never been used
94 to measure low H_2O_2 concentrations, even with pulse methods.

95 The objective of this study was to test the effectiveness of a novel method,
96 differential pulsed polarography, for quantifying H_2O_2 in slightly acidic, turbid
97 solutions with low H_2O_2 concentrations (in the mmol L^{-1} to $\mu\text{mol L}^{-1}$ range)
98 and in the presence of interfering Fe^{3+} ions or dissolved O_2 and validate its
99 application in AOPs that rely on Fenton and electro-Fenton processes. This
100 novel method reliably quantifies H_2O_2 at concentrations that are generally found
101 in Fenton reactions, and thus provides a new way of developing and optimizing
102 Fenton processes by H_2O_2 quantification. The main advantage of this method is
103 that it is very selective and avoids the interference of other compounds that may
104 be present in the solution or formed during Fenton and electro-Fenton processes.

105 2. Materials and Methods

106 2.1. Materials

107 Hydrogen peroxide (H_2O_2 , 50 % *w/v* stabilized in water), iron(III) chloride
108 (FeCl_3 , $\geq 99\%$), sulfuric acid (H_2SO_4 , 95 – 97%), sodium sulfate (Na_2SO_4 ,
109 99%), potassium iodide (KI, ACS reagent, $\geq 99\%$), ammonium molybdate
110 tetrahydrate ($(\text{NH}_4)_6\text{Mo}_7\text{O}_{24} \cdot 4\text{H}_2\text{O}$, $\geq 99\%$) and 2,9-dimethyl-1,10-phenan-
111 throline ($\text{C}_{14}\text{H}_{12}\text{N}_2$, $\geq 99.5\%$) were obtained from Sigma-Aldrich. Pure (tri-
112 distilled) mercury used for polarography was obtained from Ophram Labora-
113 toire.

114 2.2. Details of the polarographic instrument

115 Polarograms were obtained with a polarographic Metrohm 663 VA stand
116 controlled by the autolab potentiostat/galvanostat with the IME663 interface
117 (shown in Figure 1). The following functions were controlled using the nova 1.10

118 autolab software purge (N_2 , 1.5 bar), new drop and stirrer. The electrochemical
 119 cell comprised an Ag/AgCl reference electrode, a platinum counter electrode and
 a Metrohm multimode electrode Pro used as the dropping mercury electrode.

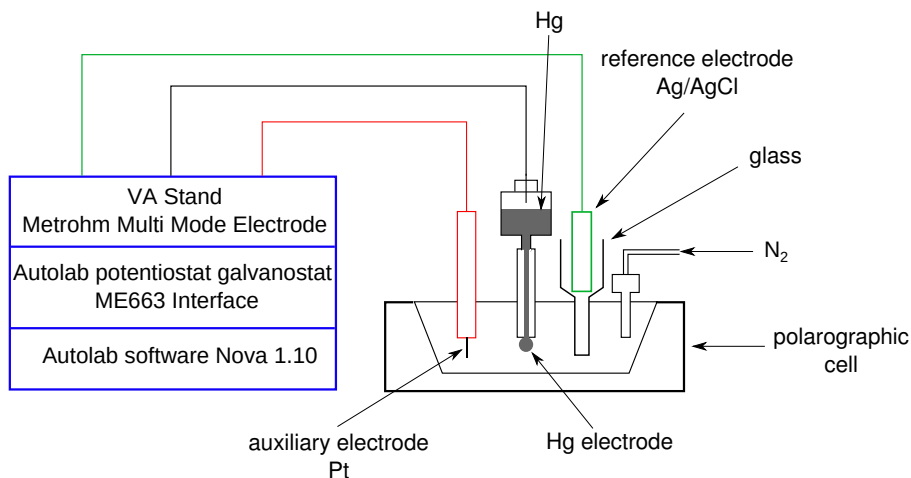
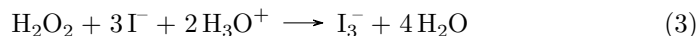


Figure 1: Diagram of the polarographic instrument.

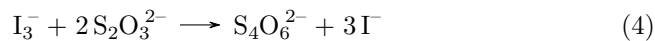
120

121 2.3. Hydrogen peroxide titration by iodometry

Hydrogen peroxide can be quantified by iodometric titration (the standard method was used here). It uses the oxidizing properties of H_2O_2 , which reacts with an excess of iodide ions to form I_3^- in an acidic environment (eq. (3)).



Ammonium molybdate was used to catalyze the reaction, but it also catalyzes oxidation by O_2 , which affect the measurements. After a 15 min wait, H_2O_2 was quantified by indirect titration of the released iodine with sodium thiosulfate $Na_2S_2O_3$ in an aqueous solution (eq. (4)). The equivalent volume was determined by adding a starch solution at end of the titration.



122 *2.4. H₂O₂ quantification using the DMP method*

The reduction of copper (II) ions by H₂O₂ in the presence of an excess of 2,9-dimethyl-1,10-phenanthroline (DMP) produces a copper(I)-DMP complex (eq. (5)) [30].



123 Copper(I)-DMP complexes can be quantified using a spectrophotometer at
124 the wavelength of its absorption maximum ($\lambda = 454 \text{ nm}$). The Shimadzu
125 1280 UV-VIS spectrophotometer was used for this measurement. The cal-
126 ibration range was $[\text{H}_2\text{O}_2] = 0.01 \text{ to } 0.50 \text{ mmol L}^{-1}$, Cu^{2+} concentration was
127 0.01 mol L^{-1} , and $[\text{DMP}] = 0.01 \text{ mol L}^{-1}$ in a phosphate buffer. The copper(II)
128 solution was prepared from a CuSO_4 powder ($\geq 99\%$) obtained from Reagent-
129 Plus. The phosphate buffer was prepared with 0.1 mol L^{-1} of K_2HPO_4 and
130 NaH_2PO_4 adjusted to $\text{pH} = 7$ by $[\text{H}_2\text{SO}_4] = 1.0 \text{ mol L}^{-1}$ and $[\text{NaOH}] = 1.0 \text{ mol L}^{-1}$.
131 The equation of the calibration curve was $y = 13.0(\pm 0.2) \times x - 0.02(\pm 0.01)$ with
132 a coefficient $R^2 = 0.999$; the determinate limit of detection (LOD) and quanti-
133 fication (LOQ) were respectively $3 \mu\text{mol L}^{-1}$ and $8 \mu\text{mol L}^{-1}$ as per Shrivastava
134 *et al.* [31].

135 *2.5. Fenton and electro-Fenton process*

136 The conditions of the Fenton process were : $[\text{H}_2\text{O}_2] = 10 \text{ mmol L}^{-1}$, $[\text{FeSO}_4] =$
137 1 mmol L^{-1} at $\text{pH} 3$ and $T = 25 \text{ }^\circ\text{C}$. The electro-Fenton experiments with a
138 three-dimensional cathode were conducted in open one-compartment PVC re-
139 actor with rectangular geometric dimensions of $14 \text{ cm (L)} \times 12 \text{ cm (l)} \times 17 \text{ cm}$
140 (H) and a volumic capacity of 1.5 L . The electrochemical reactor was equipped
141 with a compact fixed bed of glassy carbon chips and two DSA mesh anodes
142 (Ti/RuO_2) 2 cm apart [32]. The flow of the solution was perpendicular to the
143 electrodes and went through the width of the fixed bed. An air pump and an
144 air diffuser were used in the experimental setup to supply the solution contin-
145 ually with oxygen. For the quantification of hydrogen peroxide (in the absence
146 of ferrous iron) in the electro-Fenton reactor, the experimental conditions were

147 $I = 0.8$ A, flow $Q = 6$ L min⁻¹, [Na₂SO₄] = 0.05 mol L⁻¹ and pH = 3 (adjusted
148 by sulfuric acid) without the ferrous iron catalyst. Differential pulse polarogra-
149 phy (DPP) was used to study the effect of flow rate on H₂O₂ production in an
150 electro-Fenton reactor integrating a carbon monolith as the cathode material.
151 The electrochemical cell for the electro-Fenton experiments was composed of a
152 carbon monolith cylinder $\varnothing = 3.0$ cm in diameter and $d = 1.0$ cm in width as
153 working electrode, between two circular platinum plates $\varnothing = 3.0$ cm as counter
154 electrodes perforated by several holes (hole diameter = 1.5 mm) on either side
155 of the monolith cylinder. The working electrode and the counter electrodes
156 were separated by 1 mm thick rubber gaskets. Current intensity was 0.1 A. The
157 flow was regulated with a flow meter. The electro-Fenton reactor was connected
158 to a tank ($V = 2$ L) containing the reagents for the electro-Fenton process
159 : [Fe²⁺] = 0.1 mmol L⁻¹, supporting electrolyte [K₂SO₄] = 0.05 mol L⁻¹ and
160 pH 3.

161 3. Results and discussion

162 3.1. Optimisation of the pulse polarographic method

163 We assessed the impact of the variation of parameters such as drop Hg time
164 (t_g), pH and pulse amplitude ΔE on the determination of H₂O₂ in an aqueous
165 solution at the DME by differential pulse polarography.

166 DDP polarograms were recorded for blank ([Na₂SO₄] = 0.1 mol L⁻¹, pH = 3)
167 and [H₂O₂] = 200 μ mol L⁻¹ samples at different pulse amplitudes ranging from
168 -5 to -100 mV (Figure 2). A broad peak at $E_p = -1.0$ V/_{Ag/AgCl} correspond-
169 ing to the reduction of hydrogen peroxide (eq. (2)) was observed. Peak current
170 intensity (I_{pc}) as well as peak area (A_p), increased linearly with the increase
171 in ΔE for values ≤ -100 mV (Figure 3a). *I.e.* the higher the ΔE value, the
172 greater the deviation in the intensity measured (corresponding to the peak of
173 the reduction wave). This is therefore consistent with the increase in intensity
174 observed during the experiment.

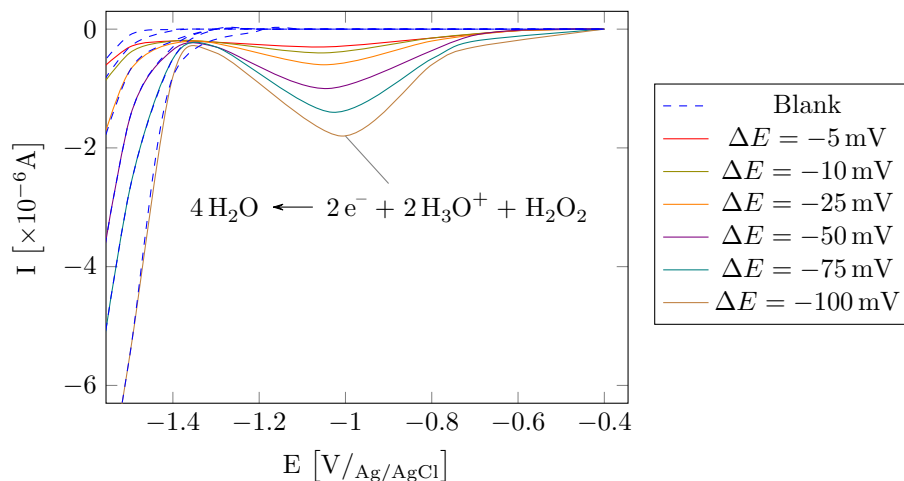


Figure 2: Differential pulse polarogram for $[\text{H}_2\text{O}_2] = 200 \mu\text{mol L}^{-1}$ in $[\text{Na}_2\text{SO}_4] = 0.1 \text{ mol L}^{-1}$, $\text{pH} = 3$ at the DME, $v = 10 \text{ mV s}^{-1}$, $t_g = 0.5 \text{ s}$, with $\Delta E = -5, -10, -25, -50, -75$ and -100 mV .

175 Moreover, the width at half height ($W_{1/2}$) of the reduction peak of H_2O_2
 176 (Figure 3b) increased slightly with ΔE variation for $\Delta E \leq 100 \text{ mV}$ and more
 177 significantly for higher values of ΔE . A significant increase in sensitivity was ob-
 178 served when large pulse amplitudes were used but when ΔE values were greater
 179 than -100 mV , peaks were broader and selectivity was affected. Therefore, a
 180 $\Delta E = -100 \text{ mV}$ appears to be a good compromise for optimal sensitivity and
 181 sufficient selectivity.

182 With increased drop time, the surface of the mercury drop was larger and
 183 consequently A_p and I_{pc} increased proportionally (shown in Figure A.1 (supple-
 184 mentary materials)). To obtain a good sensitivity level, a drop time of 1 s was
 185 chosen, corresponding to a low mercury consumption and a drop time that is
 186 not too close to the natural drop time.

187 The influence of the pH was assessed by varying the pH between 1 and
 188 9. For $\text{pH} = 1$, no peak was observed. The highest, intensity (and area) of the
 189 reduction peak was observed for $\text{pH} = 3$ (Figure 4), which is also the optimal
 190 pH for the Fenton reaction [20]. When the pH is acidic, the reduction of H_2O_2

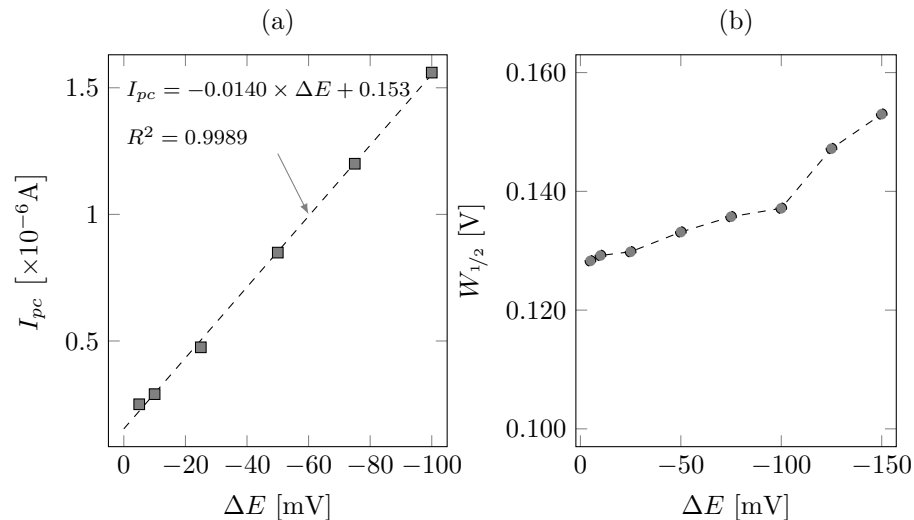


Figure 3: Evolution of (a) the peak current intensity I_{pc} ; and (b) the width of the half-peak ($W_{1/2}$) for different ΔE applied in DPP for a solution of $[H_2O_2] = 200 \mu mol L^{-1}$ in $[Na_2SO_4] = 0.1 mol L^{-1}$ at $pH = 3$.

191 involves H_3O^+ protons. Thus, a higher signal at $pH = 3$ may be due to a greater
 192 presence of H_3O^+ protons. Therefore, H_2O_2 concentration can be detected by
 193 adjusting pH conditions.

194 Thus, the optimal parameters for quantifying H_2O_2 and for obtaining have
 195 the most sensitive signal were $\Delta E = -100 mV$, $v = 10 mV s^{-1}$, $t_g = 1.0 s$ and
 196 $pH = 3$.

197 3.2. Validation of the DPP method for the determination of H_2O_2

198 Calibration, repeatability, accuracy and selectivity were considered for the
 199 validation of H_2O_2 determination by the DPP method developed here [33, 34].

200 3.2.1. Calibration curve

201 Measurements in DPP were performed for concentration of H_2O_2 ranging
 202 from 0.02 to $1.0 mmol L^{-1}$. Figure 5 shows the calibration curves for the peak
 203 current intensity (I_{pc}) and peak area (A_p) for the reduction of H_2O_2 . The
 204 fit of the linear model was good with $R^2 > 0,999$. The relationship between

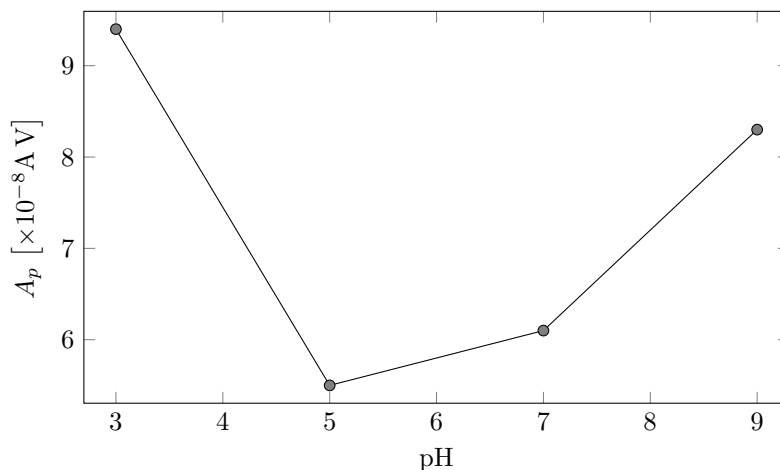


Figure 4: Evolution of the peak area A_p for pH = 3 to 9 (adjusted by H_2SO_4 and NaOH) in DPP with $[\text{H}_2\text{O}_2] = 1 \text{ mmol L}^{-1}$, $[\text{Na}_2\text{SO}_4] = 0.1 \text{ mol L}^{-1}$, $v = 10 \text{ mV s}^{-1}$, $t_g = 1.0 \text{ s}$, $\Delta E = -100 \text{ mV}$.

205 peak area and H_2O_2 concentration was linear within the 0.02 to 1 mmol L^{-1}
 206 range. For peak current intensity the linear range was slightly narrower (0.02
 207 to 0.6 mmol L^{-1}) due to the broadening of the peak at higher concentrations
 208 ($> 0.6 \text{ mmol L}^{-1}$).

209 The limit of detection ($LOD = (3.3 \times \sigma)/s$) and quantification ($LOQ = (10 \times \sigma)/s$)
 210 were calculated, where σ is the standard deviation of the regression line and s its
 211 slope (Table 1) [31]. The LOD and LOQ for the calibration curve established
 212 with A_p (respectively 13 and $40 \text{ } \mu\text{mol L}^{-1}$) are lower than the values determined
 213 with I_{pc} . Thus, for the determination of H_2O_2 concentrations in synthetic so-
 214 lutions, A_p measurements give a wider range and lower limits of detection and
 215 quantification.

216 3.2.2. Repeatability

217 Repeatability from 10 successive measurements with a $[\text{H}_2\text{O}_2] = 200 \text{ } \mu\text{mol L}^{-1}$
 218 using the A_p and I_{pc} values obtained with the DPP method developed here. The
 219 coefficient of variation (CV) was determined from eq. (6), with \bar{X} the average
 220 measurement values and s the standard deviation.

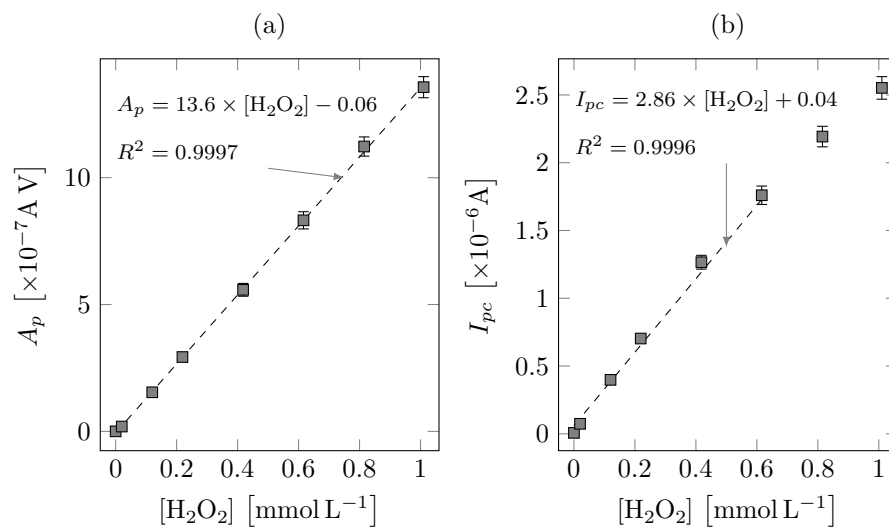


Figure 5: Calibration curves for the determination of $[H_2O_2]$ by DPP in $[Na_2SO_4] = 0.1 mol L^{-1}$, $pH = 3$, at DME with $t_g = 1.0 s$, $\Delta E = -100 mV$, $v = 10 mV s^{-1}$ (a) for the peak area (A_p) (b) for the peak current intensity (I_{pc}).

Table 1: Determination of LOD and LOQ for the calibration curves of H_2O_2 with the DPP method.

	A_p	I_{pc}
LOD ($\mu mol L^{-1}$)	13	26
LOQ ($\mu mol L^{-1}$)	40	78

$$CV(\%) = \frac{s}{\bar{X}} \times 100 \quad (6)$$

221 Results are reported in Table 2. CV values were very low, respectively
 222 around 1 % and 3 % for A_p and I_{pc} measurements, indicating a good level of re-
 223 peatability of the measurements of H_2O_2 concentration using the DPP method.

Table 2: Repeatability parameters for H_2O_2 quantification by the DPP method (from A_p and I_{pc}) applied to a 0.1 mol L^{-1} Na_2SO_4 solution with the addition of 0.2 mmol L^{-1} H_2O_2 .

	A_p	I_p
Number of assays	10	10
Mean (\bar{X}) (mmol L^{-1})	0.207	0.203
Standard deviation (s) (mmol L^{-1})	0.002	0.005
CV (%)	1.0	2.5

224 3.2.3. Trueness

225 To assess trueness study, three solutions were prepared from a H_2O_2 stock
 226 solution to cover the concentration range of the calibration curve. Expected
 227 concentration values, X , were calculated to be 0.100, 0.500 and $0.990 \text{ mmol L}^{-1}$.

228 Iodometry was used as the reference method and H_2O_2 concentrations were
 229 determined using the DPP method from the calibration curves with A_p and
 230 I_{pc} measurements. Table 3 shows the data with the recovery rate (R) equal
 231 to $R(\%) = \frac{\bar{m}}{X} \times 100$ with \bar{m} the average value of the H_2O_2 concentration
 232 measured 3 times and X the expected value of the H_2O_2 concentration. For
 233 medium (0.5 mmol L^{-1}) or high (0.99 mmol L^{-1}) concentrations, the recovery
 234 was found to be acceptable and close to 100 % (between 103 % and 90 % depend-
 235 ing on the method). Moreover, when the concentration was close to the LOQ
 236 (0.1 mmol L^{-1}), the iodometric method was not the most suitable ($R = 50 \%$),
 237 whereas recovery using the polarographic method with the peak area measure-
 238 ment was higher ($R \approx 79 \%$). This difference can be explained by the decompo-
 239 sition of H_2O_2 in water prior to the analysis when concentrations are low [35].

240 Thus, the DPP electrochemical method developed here has good accuracy even
 241 when H_2O_2 concentration values are close to the limit of quantification.

Table 3: Recovery R for iodometric titration, DPP A_p (peak area), DPP I_p (intensity) for 3 concentrations of H_2O_2 (\bar{m} : mean for 3 measurements, σ : standard deviation et R : recovery rate).

X (mmol L^{-1})		0.100	0.500	0.990
		± 0.004	± 0.002	± 0.002
Iodometric	\bar{m} (mmol L^{-1})	0.0502	0.512	0.890
	σ (mmol L^{-1})	0.0031	0.025	0.033
	R (%)	50.3	102.9	89.9
DPP A_p	\bar{m} (mmol L^{-1})	0.0787	0.483	0.878
	σ (mmol L^{-1})	0.0024	0.025	0.018
	R (%)	78.8	97.1	88.7
DPP I_{pc}	\bar{m} (mmol L^{-1})	0.0692	0.489	0.940
	σ (mmol L^{-1})	0.0019	0.009	0.011
	R (%)	69.3	98.4	95.0

242 Moreover, the standard deviation was found to be lower for the DPP method
 243 than the iodometric method. Thus, the electrochemical method developed here
 244 is more accurate and repeatable.

245 3.2.4. Selectivity

246 Selectivity is the ability of a method to perform a measurement in a com-
 247 plex matrix (presence of ions, metals, molecules). To test the selectivity of the
 248 method developed here, in particular in the context of applications under the
 249 conditions of Fenton and electro-Fenton processes, measurements of H_2O_2 con-
 250 centration were carried out in a solution containing Fe^{3+} , which can be reduced
 251 at the DME and interfere with the H_2O_2 reduction peak. Increased amounts of
 252 H_2O_2 were added to a 0.1 mol L^{-1} Na_2SO_4 solution at pH 3 with 1 mmol L^{-1}
 253 Fe^{3+} . DPP was carried out at the optimal conditions for the determination of

254 H_2O_2 concentration.

255 The differential pulse polarograms obtained for FeCl_3 with and without the
256 successive addition of H_2O_2 (0.01 to 1.0 mmol L^{-1}) are reported in Figure 6.

257 Two reduction peaks were found at :

258 • $-1.0 \text{ V}/_{\text{Ag}/\text{AgCl}}$ corresponding to the reduction of H_2O_2 to H_2O ;

259 • $-1.35 \text{ V}/_{\text{Ag}/\text{AgCl}}$ corresponding to the reduction of Fe^{3+} to Fe^{2+} .

260 These peak potentials are sufficiently spaced (350 mV) thus there is no signif-
261 icant overlap, notably for H_2O_2 concentrations $\leq 2 \text{ mmol L}^{-1}$. Moreover, at
262 higher concentrations a weak overlap appears, which does not impact the I_{pc}
263 measurement but which makes it difficult to determine A_p . Although our pre-
264 vious results suggest it is preferable to carry out the analysis of H_2O_2 from the
265 A_p measurement, it appears more appropriate to measure I_{pc} in the presence of
266 Fe^{3+} .

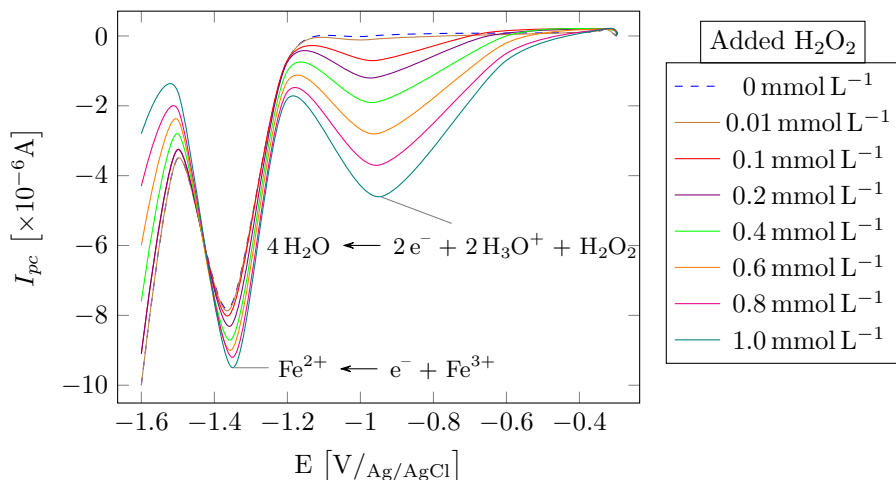


Figure 6: Differential polarograms of a solution of $[\text{Fe}^{3+}]$ (1 mmol L^{-1}) in $[\text{Na}_2\text{SO}_4] = 0.1 \text{ mmol L}^{-1}$, $\text{pH} = 3$ with successive additions of H_2O_2 (0.01 to 1 mmol L^{-1}) at the DME with $t_g = 1.0 \text{ s}$, $\Delta E = -100 \text{ mV}$, $v = 10 \text{ mV s}^{-1}$.

267 In the presence of Fe^{3+} , a good linearity was obtained for the calibration
268 curve (Figure 7), which was perfectly superimposed on the calibration line in
269 the absence of Fe^{3+} (slope deviation less than 2%).

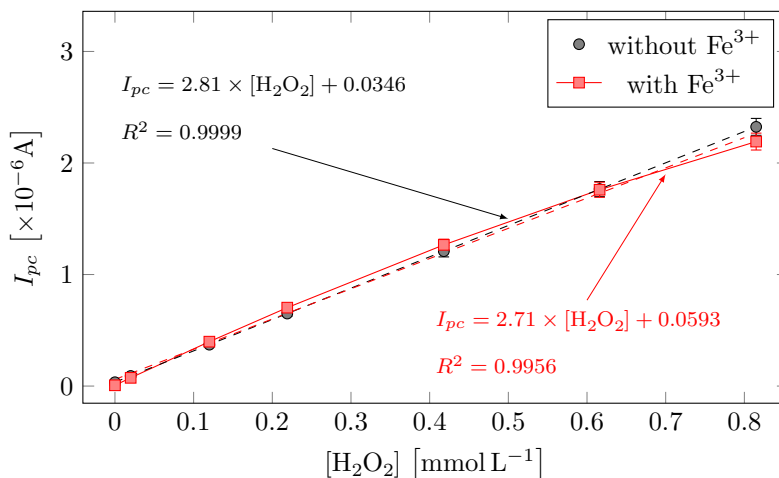


Figure 7: Comparison of calibration curves using the DPP method for measuring H_2O_2 with and without $\text{FeCl}_3 = 1 \text{ mmol L}^{-1}$ in a 0.1 mol L^{-1} Na_2SO_4 solution $\text{pH} = 3$; at the DME with $t_g = 1.0 \text{ s}$, $\Delta E = -100 \text{ mV}$, $v = 10 \text{ mV s}^{-1}$.

270 As the electrolyte (technical grade Na_2SO_4 salts) was not sufficiently pure,
 271 another interferent was identified : Zn^{2+} . Figure 8 presents several polarograms
 272 without Zn^{2+} (K_2SO_4 and $\text{K}_2\text{SO}_4 + \text{H}_2\text{O}_2$) and with the addition of Zn^{2+} in
 273 solution. A peak corresponding to Zn^{2+} reduction was observed at near the
 274 H_2O_2 reduction peak. The presence of Zn^{2+} can distort the measurements and
 275 overestimate the concentration of H_2O_2 in the solution. It is therefore necessary
 276 to carry out the DPP method without Zn^{2+} in the solution (salt purity) or use
 277 a zinc-specific complexing agent before carrying out the DPP method.

278 3.3. Hydrogen peroxide quantification in Fenton and electro-Fenton processes

279 The kinetic study of the Fenton reaction between Fe^{2+} and H_2O_2 in Fenton
 280 process experiments (section 2.5) showed after 10 min the residual concentration
 281 of H_2O_2 was lower than 1 mmol L^{-1} , which is in the same order of magnitude as
 282 the H_2O_2 concentrations during the production of H_2O_2 by the electro-Fenton
 283 process, as observed here. Figure 9 shows H_2O_2 concentration over time, after
 284 10 min of the Fenton reaction, as measured by two quantification methods :
 285 iodometric titration and the DPP method using I_{pc} .

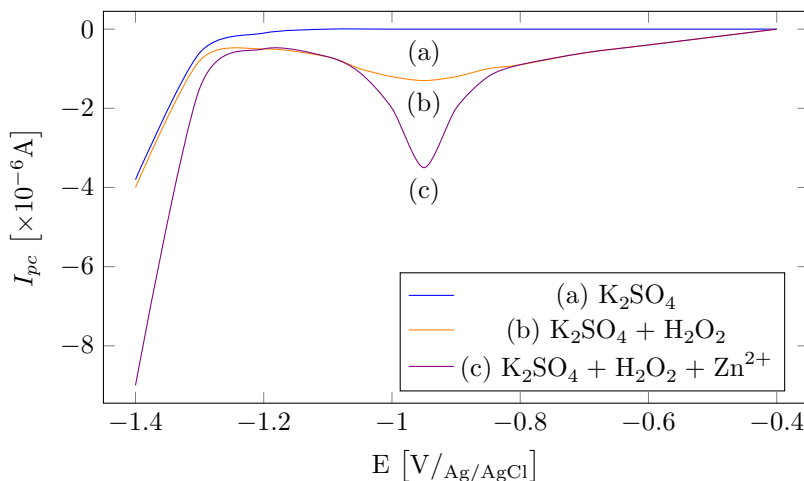


Figure 8: Polarograms of an electrolyte solution support ($[\text{K}_2\text{SO}_4] = 0.1 \text{ mol L}^{-1}$) (a), with H_2O_2 (1.0 mmol L^{-1}) (b) and with the addition of Zn^{2+} (0.1 mmol L^{-1}) (c).

286 The DPP method could determine significantly lower H_2O_2 concentrations
 287 than the iodometric method. The observed difference between these two meth-
 288 ods was more important than during the electro-Fenton process (approxima-
 289 tively 0.20 mmol L^{-1} vs. 0.07 mmol L^{-1}). In addition to the previously dis-
 290 cussed interference of dissolved O_2 in the iodometric method, the presence of
 291 Fe^{3+} resulting from the Fenton reaction can promote a reaction with the titrated
 292 reagent $\text{S}_2\text{O}_3^{2-}$ and overestimate the concentration of H_2O_2 . By contrast, in the
 293 DPP method, the presence of Fe^{3+} does not interfere with the determination of
 294 H_2O_2 concentration.

295 The optimized DPP method for H_2O_2 determination was applied to Fenton
 296 and electro-Fenton processes in reactors developed in the laboratory [32, 36] for
 297 the treatment of organic micropollutants. For the electro-Fenton process with
 298 a three-dimensional cathode composed of a fixed bed of packed electrodes (see
 299 section 2.5), experiments were conducted without an Fe^{2+} catalyst to evaluate
 300 the production of H_2O_2 by dissolved oxygen at the three-dimensional cathode.
 301 The kinetics of H_2O_2 production (Figure 10) were determined by iodometric

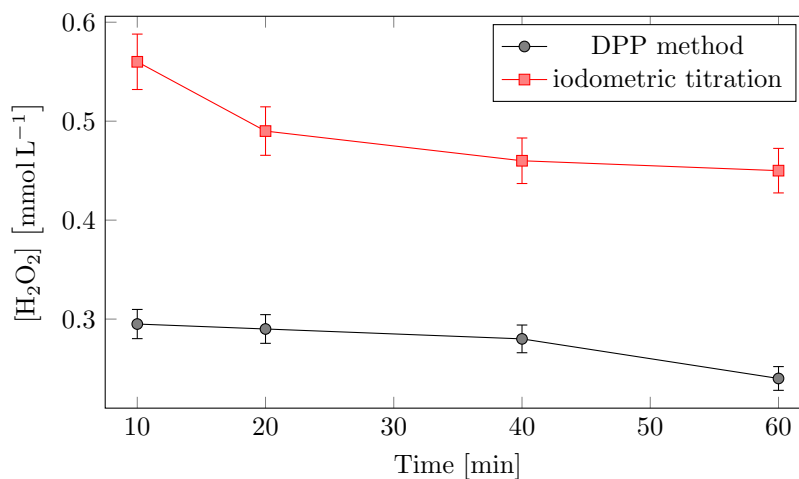


Figure 9: Comparison of iodometric titration and DPP for H₂O₂ determination after 10 min of the Fenton reaction : [H₂O₂] = 10 mmol L⁻¹ at $t = 0$ min, [FeSO₄] = 1 mmol L⁻¹ at pH 3.

302 titration and DPP with external calibration (see section 3.2.1) and standard
 303 addition (successive additions of 0.5 μ mol H₂O₂ to the sample). No difference
 304 was observed for DPP between external calibration and standard addition (devi-
 305 ation < 8 %). However, data obtained by iodometric titration have a maximum
 306 deviation of 55 % compared to the DPP method.

307 This difference can be explained by the presence of dissolved oxygen in solu-
 308 tion and the reaction of dissolved O₂ with thiosulfate when H₂O₂ concentrations
 309 are low. With the DPP method, the solution was degassed by N₂ bubbling and
 310 no interference from O₂ was observed.

311 These two experiments show that the iodometric method introduces a bias
 312 in the determination of low H₂O₂ concentrations. In order to confirm the ac-
 313 curacy of the H₂O₂ concentration measurement with the electrochemical DPP
 314 method, the DMP spectrophotometric method (section 2.4) was carried out and
 315 compared to the DPP method by studying the electro-Fenton process in a re-
 316 actor containing a carbon monolith cylinder as the cathode (section 2.5). In
 317 this type of flow cell laboratory set-up, it is important to determine the optimal
 318 flow rate for the production of H₂O₂ by electrochemical reduction of dissolved

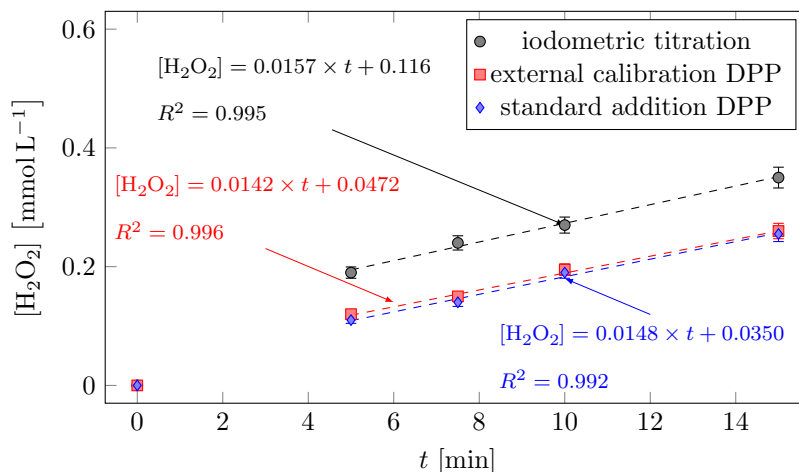


Figure 10: Comparison of iodometric titration and DPP with external calibration and standard addition for the determination methods of H_2O_2 production during the electro-Fenton process.

319 oxygen. Thus, H_2O_2 concentrations after 2 hours of electrolysis with different
 320 flow rates (80 to 200 L min^{-1}) were determined by the two methods (DDP and
 321 DMP) and are reported in Figure 11.

322 Measurements with the DMP method were close to those obtained with the
 323 DPP method (maximum deviation of 7%). The results obtained with the DMP
 324 method confirm and validate the determination of H_2O_2 concentration by the
 325 DPP method in the electro-Fenton process experiments. Comparison of the
 326 impact of flow rate on H_2O_2 production showed that a flow rate of 140 L h^{-1}
 327 was the optimal flow rate with a H_2O_2 production of 0.38 mmol L^{-1} after 2 h of
 328 electrolysis at 0.1 A.

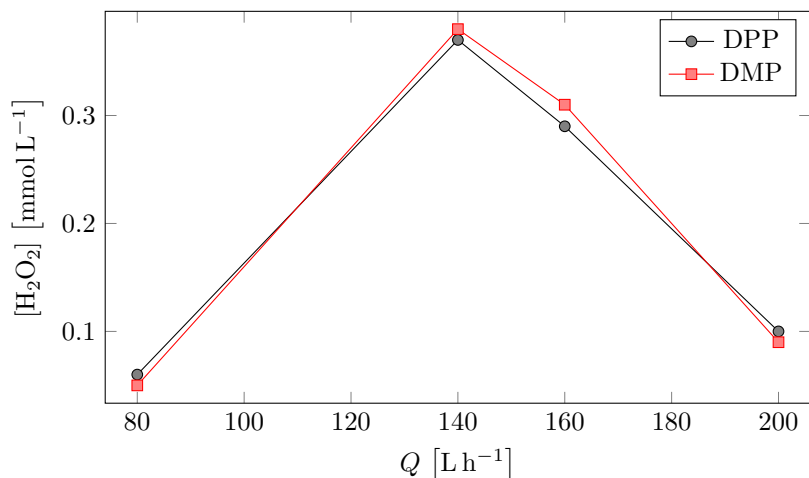


Figure 11: H₂O₂ analysis by the DMP and DPP methods during the electro-Fenton process at $t = 2$ h of electrolysis : $I = 100$ mA, $[\text{K}_2\text{SO}_4] = 0.05$ mol L⁻¹, $Q = 80, 140, 160, 200$ L h⁻¹, $pH = 3$.

329 4. Conclusion

330 We have developed a differential pulse polarographic (DPP) method to de-
 331 termine H₂O₂ concentration. The external calibration curve was obtained for
 332 low H₂O₂ concentrations between 0.02 and 1 mmol L⁻¹. This method has a
 333 good sensitivity with limits of detection and quantification respectively at 13
 334 and 40 μmol L⁻¹. Moreover, the DPP method is selective in the presence of
 335 Fe³⁺ (Fenton reaction) which is an interfering species in the iodometric method.
 336 However, measurements can be distorted by the presence of traces of Zn²⁺ in
 337 solution because its peak current occurs at the same potential as H₂O₂. This
 338 can be a problem especially for the determination of H₂O₂ in industry because
 339 metal corrosion (valves, pumps, ...) could release Zn²⁺ ions in the solution.
 340 To eliminate this interference, it is possible to add a zinc-specific complexing
 341 agent to the sample before applying the DPP method. The DPP method for the
 342 quantification of H₂O₂ from the Fenton reaction and the electro-Fenton process
 343 was compared to other titration methods (iodometric and DMP). Iodometric
 344 titration appears unsuitable for low concentrations of H₂O₂ in the presence of

345 O₂ dissolved in solution (electro-Fenton process) and in the presence of Fe³⁺
346 (Fenton reaction), unlike the DPP electrochemical method. To conclude, the
347 DPP method developed here to quantify H₂O₂ in a process implying the Fenton
348 reaction is usable, selective and precise at low concentrations in the range of the
349 mmol L⁻¹ or lower, and can be conducted in solutions containing O₂ and Fe³⁺.

350 **Conflicts of interest**

351 There are no conflicts to declare.

A. Supplementary Materials

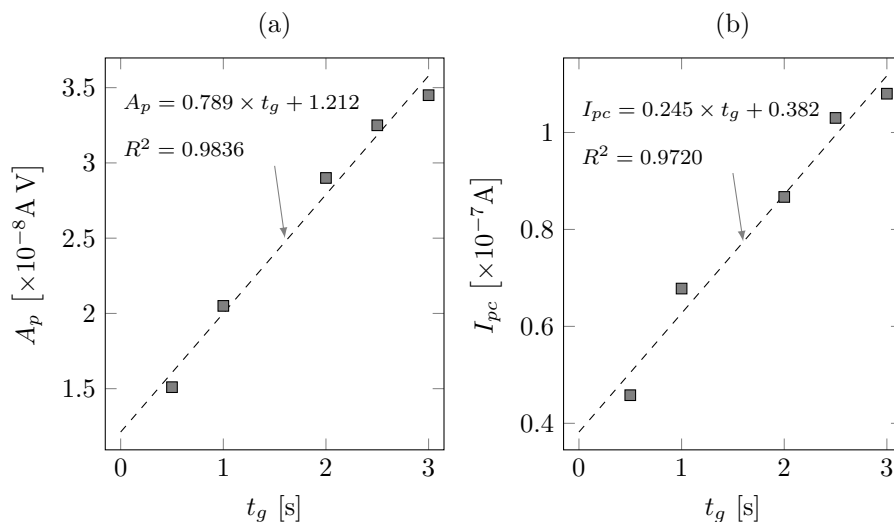


Figure A.1: Evolution of (a) the peak area A_p ; and (b) the peak current intensity I_{pc} at different mercury drop time t_g applied in DPP for a solution of $[\text{H}_2\text{O}_2] = 200 \mu\text{mol L}^{-1}$ in $[\text{Na}_2\text{SO}_4] = 0.1 \text{ mol L}^{-1}$ at $\text{pH} = 3$.

References

- [1] J.-H. Sun, S.-P. Sun, G.-L. Wang, L.-P. Qiao, Degradation of azo dye amido black 10b in aqueous solution by fenton oxidation process, *Dyes and Pigments* 74 (3) (2007) 647–652.
- [2] S. Mishra, B. Sundaram, S. Muthukumar, Advanced oxidation process for leachate treatment: A critical review (2022). doi:10.1201/9781003165958-14.
- [3] J. A. Garrido-Cardenas, B. Esteban-García, A. Agüera, J. A. Sánchez-Pérez, F. Manzano-Agugliaro, Wastewater treatment by advanced oxidation process and their worldwide research trends, *International Journal of Environmental Research and Public Health* 17 (1) (2020) 170.

- 364 [4] E. Neyens, J. Baeyens, A review of classic fenton and peroxidation as an
365 advanced oxidation technique, *Journal of Hazardous materials* 98 (1) (2003)
366 33–50.
- 367 [5] M. Perez, F. Torrades, J. A. Garcia-Hortal, X. Domenech, J. Peral, Re-
368 moval of organic contaminants in paper pulp treatment effluents under
369 fenton and photo-fenton conditions, *Applied Catalysis B: Environmental*
370 36 (1) (2002) 63–74.
- 371 [6] K. Chan, W. Chu, Modeling the reaction kinetics of fenton process on the
372 removal of atrazine, *Chemosphere* 51 (4) (2003) 305–311.
- 373 [7] H. Luo, Y. Zeng, D. He, X. Pan, Application of iron-based materials in
374 heterogeneous advanced oxidation processes for wastewater treatment: A
375 review, *Chemical Engineering Journal* 407 (2021) 127191.
- 376 [8] F. Zaviska, P. Drogui, G. Mercier, J.-F. Blais, Procédés d’oxydation avancée
377 dans le traitement des eaux et des effluents industriels: Application à la
378 dégradation des polluants réfractaires, *Revue des sciences de l’eau/Journal*
379 *of Water Science* 22 (4) (2009) 535–564.
- 380 [9] S. O. Ganiyu, C. A. Martínez-Huitle, M. A. Oturan, Electrochemical ad-
381 vanced oxidation processes for wastewater treatment: Advances in forma-
382 tion and detection of reactive species and mechanisms, *Current Opinion in*
383 *Electrochemistry* 27 (2021) 100678.
- 384 [10] L. Liu, Z. Chen, J. Zhang, D. Shan, Y. Wu, L. Bai, B. Wang, Treatment
385 of industrial dye wastewater and pharmaceutical residue wastewater by
386 advanced oxidation processes and its combination with nanocatalysts: A
387 review, *Journal of Water Process Engineering* 42 (2021) 102122.
- 388 [11] M.-h. Zhang, H. Dong, L. Zhao, D.-x. Wang, D. Meng, A review on fenton
389 process for organic wastewater treatment based on optimization perspec-
390 tive, *Science of the Total Environment* 670 (2019) 110–121.

- 391 [12] E. Brillas, I. Sirés, M. A. Oturan, Electro-fenton process and related elec-
392 trochemical technologies based on fenton's reaction chemistry, *Chemical*
393 *reviews* 109 (12) (2009) 6570–6631.
- 394 [13] J. Casado, Towards industrial implementation of electro-fenton and derived
395 technologies for wastewater treatment: A review, *Journal of Environmental*
396 *Chemical Engineering* 7 (1) (2019) 102823.
- 397 [14] Z. Deng, L. Zhao, H. Zhou, X. Xu, W. Zheng, Recent advances in electro-
398 chemical analysis of hydrogen peroxide towards in vivo detection, *Process*
399 *Biochemistry* 115 (2022) 57–69. doi:10.1016/j.procbio.2022.01.025.
- 400 [15] M. Song, J. Wang, B. Chen, L. Wang, A facile, non-reactive
401 hydrogen peroxide detection method enabled by ion chromatogra-
402 phy with uv detector., *Analytical chemistry* 89 (2017) 11537–11544.
403 doi:10.1021/acs.analchem.7b02831.
- 404 [16] M. Baghayeri, H. Alinezhad, M. Tarahomi, M. Fayazi, M. Ghanei-Motlagh,
405 B. Maleki, A non-enzymatic hydrogen peroxide sensor based on dendrimer
406 functionalized magnetic graphene oxide decorated with palladium nanopar-
407 ticles, *Applied Surface Science* 478 (2019) 87–93.
- 408 [17] C. Liang, B. He, A titration method for determining individual oxidant con-
409 centration in the dual sodium persulfate and hydrogen peroxide oxidation
410 system, *Chemosphere* 198 (2018) 297–302.
- 411 [18] J. Rodier, B. Legube, *L'analyse de l'eau*, Dunod, 2009.
- 412 [19] K. Kosaka, H. Yamada, S. Matsui, S. Echigo, K. Shishida, Comparison
413 among the methods for hydrogen peroxide measurements to evaluate ad-
414 vanced oxidation processes: application of a spectrophotometric method
415 using copper (ii) ion and 2, 9-dimethyl-1, 10-phenanthroline, *Environmental*
416 *Science & Technology* 32 (23) (1998) 3821–3824.

- 417 [20] A. Babuponnusami, K. Muthukumar, A review on fenton and improve-
418 ments to the fenton process for wastewater treatment, *Journal of Environ-*
419 *mental Chemical Engineering* 2 (1) (2014) 557–572.
- 420 [21] J. Reichert, S. McNeight, H. Rudel, Determination of hydrogen peroxide
421 and some related peroxygen compounds, *Industrial & Engineering Chem-*
422 *istry Analytical Edition* 11 (4) (1939) 194–197.
- 423 [22] D. Wang, S. Qiu, M. Wang, S. Pan, H. Ma, J. Zou, Spectrophotometric
424 determination of hydrogen peroxide in water by oxidative decolorization of
425 azo dyes using fenton system, *Spectrochimica Acta Part A: Molecular and*
426 *Biomolecular Spectroscopy* 221 (2019) 117138.
- 427 [23] T. Brennan, C. Frenkel, Involvement of hydrogen peroxide in the regulation
428 of senescence in pear, *Plant Physiology* 59 (3) (1977) 411–416.
- 429 [24] J. Lin, J. Xiao, H. Cai, Y. Huang, J. Li, H. Yang, T. Li, J. Zou, Multi-
430 wavelength spectrophotometric determination of peracetic acid and the co-
431 existent hydrogen peroxide via oxidative coloration of abts with the assis-
432 tance of Fe^{2+} and KI , *Chemosphere* 287 (2022) 132242.
- 433 [25] R. F. P. Nogueira, M. C. Oliveira, W. C. Paterlini, Simple and fast spec-
434 trophotometric determination of H_2O_2 in photo-fenton reactions using meta-
435 vanadate, *Talanta* 66 (1) (2005) 86–91.
- 436 [26] M. Heyrovský, Polarography—past, present, and future, *Journal of Solid*
437 *State Electrochemistry* 15 (2011) 1799–1803.
- 438 [27] M.-L. Abasq, P. Courtel, G. Burgot, Determination of entacapone by differ-
439 ential pulse polarography in pharmaceutical formulation, *Analytical letters*
440 41 (1) (2008) 56–65.
- 441 [28] H. Y. Ahmed, S. B. Dikran, S. A. Al-Ameri, Determination of ibuprofen
442 in pharmaceutical formulations using differential pulse polarography, *Ibn*
443 *AL-Haitham Journal For Pure and Applied Science* 32 (3) (2019) 56–61.

- 444 [29] D. Hauchard, Polarographie techniques polarographiques en analyse, Tech-
445 niques de l'ingénieur Méthodes électrochimiques base documentaire :
446 TIB388DUO. (ref. article : p2135), fre (2008). arXiv:base documentaire
447 : TIB388DUO.
- 448 [30] E. Illés, A. Tegze, K. Kovács, G. Sági, Z. Papp, E. Takács, L. Wojnárovits,
449 Hydrogen peroxide formation during radiolysis of aerated aqueous solutions
450 of organic molecules, *Radiation Physics and Chemistry* 134 (2017) 8 – 13.
451 doi:<https://doi.org/10.1016/j.radphyschem.2016.12.023>.
- 452 [31] A. Shrivastava, V. B. Gupta, et al., Methods for the determination of limit
453 of detection and limit of quantitation of the analytical methods, *Chronicles*
454 of young scientists 2 (1) (2011) 21–25.
- 455 [32] A. Chmaysem, S. Taha, D. Hauchard, Scaled-up electrochemical reactor
456 with a fixed bed three-dimensional cathode for electro-fenton process: ap-
457 plication to the treatment of bisphenol a, *Electrochimica Acta* 225 (2017)
458 435–442.
- 459 [33] I. S. Committee, et al., Validation of analytical procedures: Text and
460 methodology q2 (r1), Harmonized Tripartite Guideline (2005).
- 461 [34] A. G. González, M. Á. Herrador, A practical guide to analytical method
462 validation, including measurement uncertainty and accuracy profiles, *TrAC*
463 Trends in Analytical Chemistry 26 (3) (2007) 227–238.
- 464 [35] P. Pkedziwiatr, et al., Decomposition of hydrogen peroxide-kinetics and
465 review of chosen catalysts, *Acta Innovations* (2018) 45–52.
- 466 [36] L. Domergue, Étude de la régénération d'adsorbants par oxydation indi-
467 recte, Ph.D. thesis, Université Rennes 1 (2019).